Ultrasonics Sonochemistry 74 (2021) 105577

Contents lists available at ScienceDirect

Ultrasonics Sonochemistry

journal homepage: www.elsevier.com/locate/ultson

Circular motion of submillimeter-sized acoustic bubbles attached to a boundary by high-speed image analysis

Bai Lichun[a], Sun Jinguang[a,*], Gao Yandong[a], Xu Weilin[b,*], Zeng Zhije[c], Ma Yuhang[c], Bai Lixin[c,d,*]

[a] School of Electronic and Information Engineering, Liaoning Technical University, Huludao 125105, China
[b] State Key Laboratory of Hydraulics and Mountain River Engineering, Sichuan University, Chengdu 610065, China
[c] State Key Laboratory of Acoustics, Institute of Acoustics, Chinese Academy of Sciences, Beijing 100190, China
[d] North China Electric Power University, Beijing 102206, China

ARTICLE INFO

Keywords:
Circular motion
Submillimeter-sized bubble
Acoustic field
Bubble array
High-speed photography

ABSTRACT

The circular motion of submillimeter-sized bubbles attached to a boundary in an 18.5 kHz ultrasonic field are investigated experimentally by high-speed photography and image analysis. It is found that the vibration of gas bubbles with diameters of 0.2–0.4 mm is between spherical radial vibration and regular surface fluctuation. Different from the circular motion of suspended bubbles in water, the circular motion of gas bubbles attached to a boundary presents some new characteristics. These bubbles attached to a boundary (wandering bubbles) will rotate around a fixed bubble array (holding bubbles). Both the wondering bubbles and holding bubbles are "degas" bubbles. The primary Bjerknes force acting on wandering bubbles in the acoustic wave field and the secondary Bjerknes force between the wandering bubbles and the holding bubbles strongly affects the circular motion. The circling and residence behavior of gas bubbles is described and analyzed in detail, which is helpful to understand and improve industrial applications such as ultrasonic cleaning, sonochemical treatment, aeration and cavitation reduction.

1. Introduction

Bubbles and its motion greatly affect the physical properties and flow properties of the fluid. The study of bubble motion in fluid is of great significance to ultrasonic cleaning, sonochemistry, aeration and cavitation reduction. The bubble in the fluid can not only move with the fluid, but also move relative to the fluid. For example, under the action of hydrodynamic forces, bubbles may exhibit zigzag or spiral motions in the fluid [1]. Under the action of ultrasound, bubbles in liquid may also exhibit various motions. For example, bubbles may vibrate radially [2], generate high temperature and high pressure inside the bubbles [3], and generate microstreaming in the surrounding liquid [4]; bubbles may collapse asymmetrically and produce a high-speed microjet [5,6]; the surface of bubbles may fluctuate or split [7,8]. In addition to the in-situ deformation of bubbles mentioned above, the bubbles may move translationally under the action of ultrasound. For example, under the action of the primary Bjerknes forces, bubbles may move towards the node or antinode of a standing wave field according to its relative ratio to the resonance radius [9]. Considering the nonlinear oscillation of bubbles, all bubbles will move away from the pressure antinode at high enough pressure [10]. All bubbles in a traveling wave field will move in the direction of wave propagation, except for very large or very small bubbles (the force applied to them can be ignored) [11]. Under the action of secondary Bjerknes forces, bubbles may move towards each other and eventually merge if they are oscillating in phase [12].

In addition to the cases mentioned above, bubbles may also exhibit a special translational motion in an ultrasonic field - circular motion. Miller (1977) [13] observed bubbles moving to particular locations and organizing into stable arrays in a 1 MHz standing wave acoustic field. He also noticed that, depending on their sizes, these bubbles may be trapped or experience orbital trajectories in the vicinity of the pressure node locations. He hypothesized that the interplay of size changes due to diffusion, and of changes in the radiation forces on the bubbles due to the size change could explain the circular motion. Barbat et al. (2004) [14] found after theoretical examination that two bubbles with volume oscillation may have elliptical trajectories in an inviscid system where bubbles experience no drag from surrounding liquid. They considered that bubbles may continue rotating by the force balance between

* Corresponding authors.
E-mail addresses: sjg_lntu@163.com (J. Sun), xuwl@scu.edu.cn (W. Xu), blx@mail.ioa.ac.cn (L. Bai).

https://doi.org/10.1016/j.ultsonch.2021.105577
Received 31 January 2021; Received in revised form 15 April 2021; Accepted 22 April 2021
Available online 25 April 2021

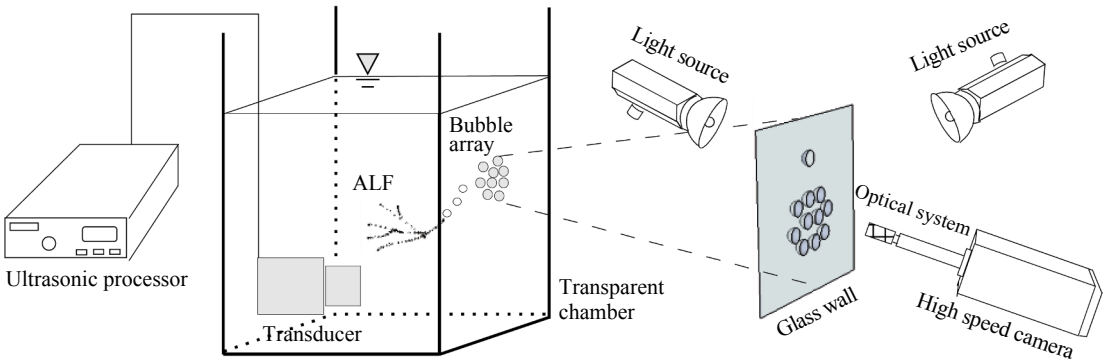

Fig. 1. Experimental setup.

repulsive centrifugal force and attractive secondary Bjerknes force acting on bubbles with in phase volume oscillations. Rensen et al. (2001) [15] investigated experimentally the effect of acoustic forces (20 kHz) on a bubble immersed in a shear flow. The experiments have demonstrated that the competition between hydrodynamic and acoustic forces can result in a spiraling motion of the bubble. Shirota et al. (2012) [16] investigated experimentally the circular motion of two oscillating bubbles in a round bottom flask with 20 kHz transducers attached on the both sides of the flask which is the same as ones commonly used for single bubble sonoluminescence experiment. They found that pairs of bubbles revolve along an elliptic orbit around the center of mass of the bubbles, and the two bubbles perform anti-phase radial oscillation. They considered that there was a centripetal primary Bjerknes force against the repulsive secondary Bjerknes force. Desjouy et al. (2013) [17] (2013) [18] found that acoustic cavitation-induced micro bubbles in a 30 kHz cylindrical resonator filled with water tend to concentrate into ring patterns due to the cylindrical geometry of the system. They considered that the shape of these ring patterns is directly linked to the Bjerknes force distribution in the resonator.

In the above literature on circular motion of gas bubble, bubbles are all suspended in the liquid [13-18], and there is nothing in the center of orbital trajectory. Different from the above studies, the present work is an investigation on gas bubbles attached to a boundary rotate around a fixed bubble array. This phenomenon sometimes appears in ultrasonic cleaning or sonochemical treatment, especially in the acoustic field with more air content. The quasi two-dimensional circular motion on the

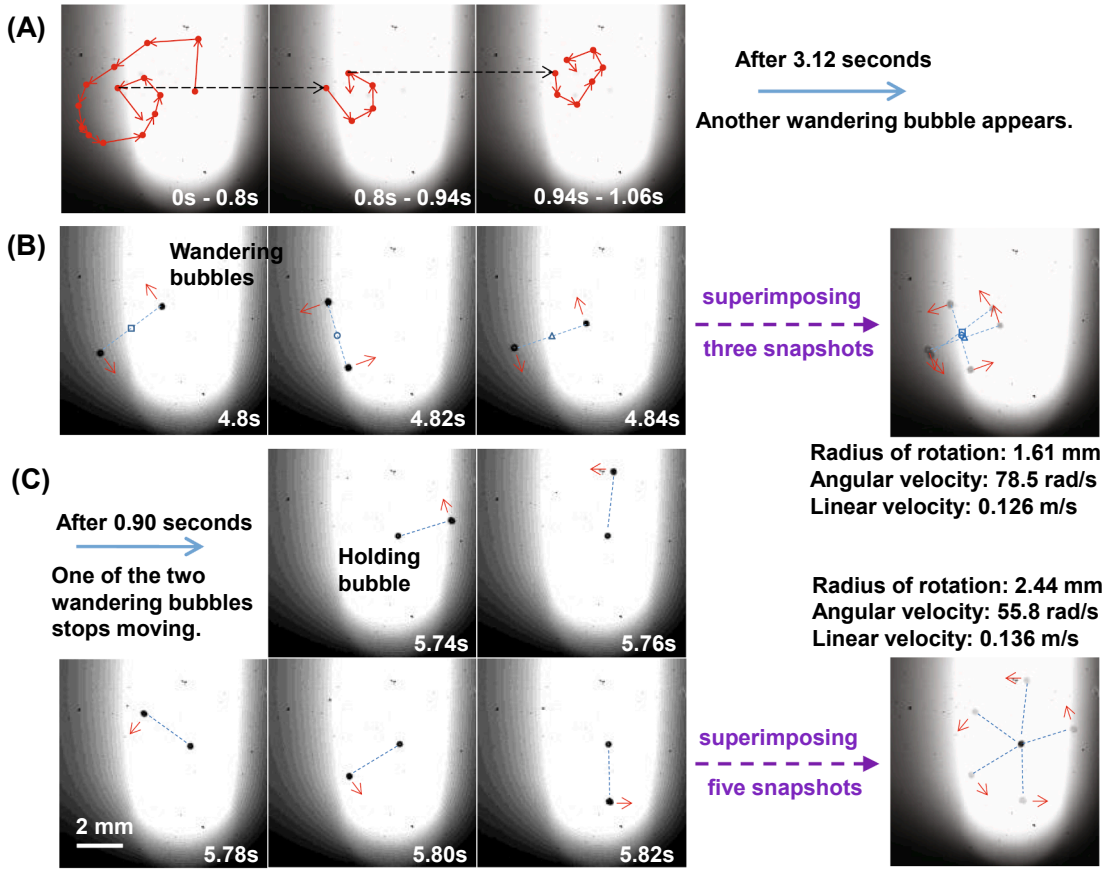

Fig. 2. Initial evolution of circular motion of gas bubbles. (A) Circular motion of one gas bubble. (B) The two bubbles rotate around the center. (C) One bubble rotates around the other bubble. The output power of ultrasonic generating system is about 50 W.

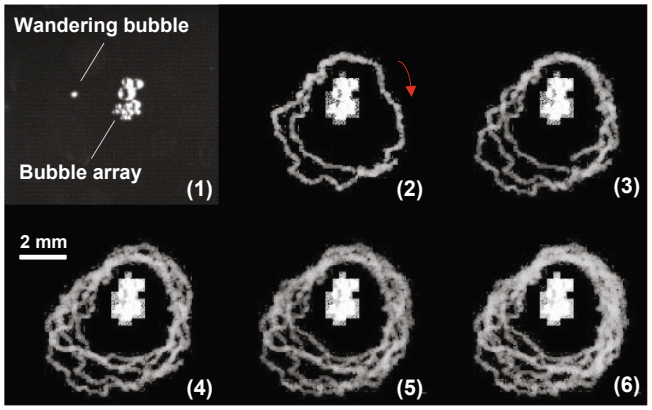

Fig. 3. Circular motion of a gas bubble around a bubble array. (A composite image of superimposing the snapshots from the video sequence) (The number of circles increases gradually.) The output power of ultrasonic generating system is about 50 W.

boundary is very suitable for the image analysis based on high-speed photography.

2. Experiment

The experimental diagram is shown in Fig. 1. The ultrasonic horn is mounted horizontally in a transparent chamber (600 mm × 330 mm × 330 mm). The piezoceramic sandwich transducers are enveloped in a shell and can be submerged in water completely. The continuous-wave ultrasound is produced by a ultrasonic processors (Jiuzhou Ultrasonic Technology Co., Ltd. China) with a frequency of 18.5 kHz (radiating surface diameter, d = 50 mm) and a maximum input electric power of 100 W (actual output power is 30–60 W). The circular motion of bubbles on the wall of transparent chamber is recorded by two high-speed cameras (Photron Fastcam SA-1, Photron Ltd., Japan; Photron Fastcam-Super 10, Photron Ltd., Japan) equipped with two long distance microscopes (Zoom 6000, Navitar, USA; 75 mm, Edmund Optics, USA) respectively. The frames are illuminated with a PI-LUMINOR high-light LED lamp (150 W) and a HALOGEN lamp (2600 W). The positions of light source (shooting angle) were adjusted for a better photographic effect. Fresh tap water (20 °C, with many nuclei) is used in the experiment so as to reduce the cavitation threshold and increase the number of wandering gas bubbles and holding bubbles attached to the boundary. The liquid height (270 mm) was adjusted as the resonance condition. When the liquid height changes, the position of the bubble array will also change.

3. Results and discussion

When the conditions remain unchanged (e.g. acoustic properties, transducer location, liquid height), circular motion of submillimeter-sized gas bubbles can be observed at some specific areas on the chamber wall (as shown in Fig. 1). Before the experiment, make sure that there are no bubbles on the chamber wall. When the transducer is turned on, the first wandering bubble moves in a circle on the wall (as shown in Fig. 2A). The mechanism of the first bubble attached to the wall rotation is the same as that of bubbles suspended in water [17]. However, when there are two wandering bubbles attached to the wall in this area, the circular motion changes greatly (as shown in Fig. 2B, about 3 s later in the same experiment). The two bubbles can wander freely along the wall, they will rotate around the center (as shown the composite image of superimposing three snapshots, τ = 4.8 s, 4.82 s and 4.84 s in Fig. 2B). Although the position of circular motion is still unstable, the diameter of the orbital trajectory is fixed. A similar study on the circular motion of two oscillating bubbles is described and analyzed in ref.[16]. The

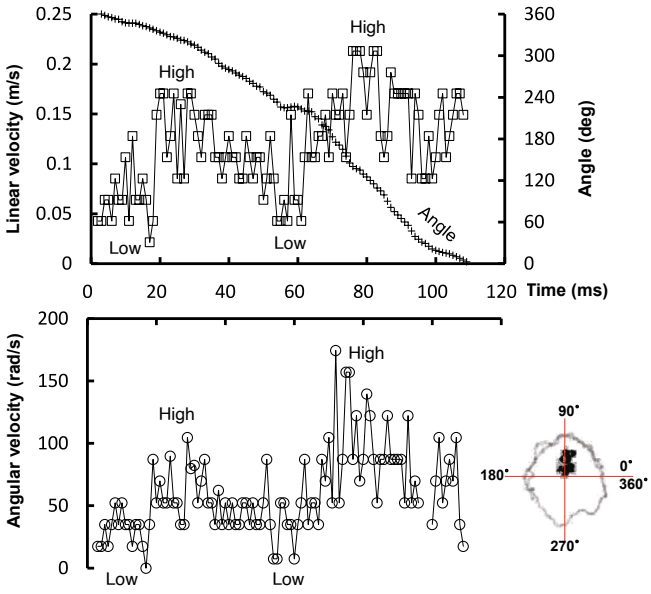

Fig. 4. The linear velocity and angular velocity of the wandering bubble in a cycle in the same experiment of Fig. 3.

circular motion of two wandering bubbles is unsustainable. One of the two bubbles tends to be fixed on the wall (holding bubble), the other bubble (wandering bubble) will rotate around it (as shown in Fig. 2C, about 1 s later in the same experiment). The holding bubble is anchored on the surface like an anchor, the behavior of the other bubble becomes more predictable. The radius of rotation and linear velocity of the circular motion increase, while the angular velocity decreases. The primary Bjerknes force drives the two bubbles to approach, while the secondary Bjerknes force drives them to separate, which ensures the stability of the distance between two bubbles. This is related to the vibration mode of the bubbles. The bubbles not only vibrates radially, but also fluctuates on the surface. The vibration phase affects the direction of the secondary Bjerknes force, which we will discuss later.

With the increase of the number of holding bubbles, a bubble array will be formed on the boundary, and wandering bubbles will rotate around the bubble array. Fig. 3 shows the trajectory of a wandering bubble motion (about 100 pictures per circle) displayed by superimposing the high-speed photography pictures (Frame rate 1000 fps). Different from the circular motion of suspended bubbles in water (regular, stable and smooth) [13-18], the orbital trajectory of wandering bubble attached to the boundary is not regular circular or elliptical (The trajectory is approximately the contour of the bubble array), the trajectory is not stable (the trajectory of each cycle does not coincide), and the trajectory is not smooth (the trajectory curve has many singular points). This is due mainly to the acoustic field radiated by the holding bubbles in the array. The spatial and size distribution of holding bubbles in the array is very complex, which makes the equilibrium position of the primary Bjerknes force and the secondary Bjerknes force very unstable and irregular. There may even be Bjerknes force potential well, where the wandering bubble is confined to a certain position and cannot continue to rotate. The shape of the bubble array and the holding bubbles on the edge of array affect the motion of wandering bubbles. The Bjerknes force on the wandering bubble is unstable due to its position change and severe deformation, which will be discussed later. The boundary effect of vibrating bubbles also plays an important role. Acoustically hard object surfaces can attract bubbles due to secondary Bjerknes forces from reflections [11] (virtual mirror bubbles [19]), and pits on the wall tend to collect and hold wandering bubbles [20]. These make the wandering bubble encounter many disturbances in the process of rotation.

It is found that the upper trajectories are approximately coincident,

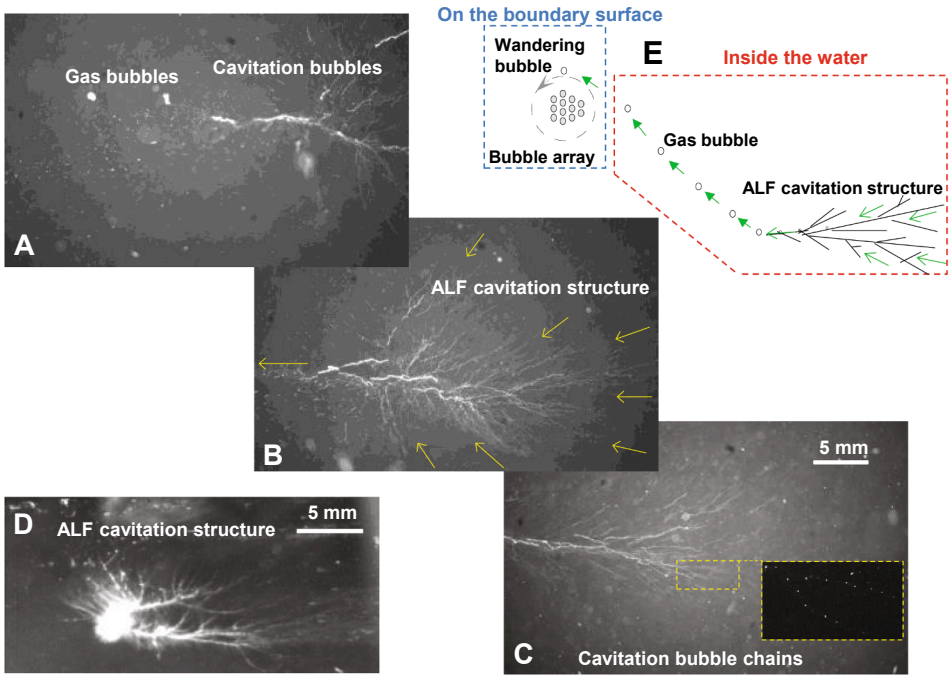

Fig. 5. The source of bubble array attached to the wall in ultrasonic field. (A) (B) (C) Front, middle and rear of ALF (Acoustic Lichtenberg Figure) cavitation structure with gas bubble generation. (D) ALF cavitation structure without gas bubble generation. (E) Schematic diagram of generation and movement of wandering bubbles. The output power of ultrasonic generating system is about 50 W.

while the lower trajectories are scattered, and the bubble array is closer to the upper part of the trajectory loop (as shown in Fig. 3(6)). This indicates that the wandering bubble is subjected to a stronger secondary Bjerknes forces with greater repulsion at the lower part. Fig. 3(1) shows that three large holding bubbles are located in the upper part of the array, while nine small holding bubbles are located in the lower part of the array. Small holding bubbles vibrate more violently and radiate stronger sound waves. The secondary Bjerknes force is stronger when the wandering bubble is close to these small holding bubbles.

Fig. 4 shows the linear velocity and angular velocity of the wandering gas bubble in a cycle. The experimental results show that the velocity of wandering bubbles is not steady. The linear velocity and angular velocity have two maximum values and two minimum values in a cycle. This implies the existence of nodal line on which bubble translation is fast due to high pressure gradient, and of anti-nodal region in which bubble translation is low but volume pulsation is great, which is consistent with the results of Shirota et al. (2012) [16].

The volume of a wandering gas bubble is about 1 / 2 to 1 / 3 of that of a holding gas bubble (0.4–1.2 mm) in the experiments. If the wandering bubble is too large, the Bjerknes forces applied to it will be very small [11]. The too large wandering bubble will not move orbitally, but will become a holding bubble or float out of the liquid surface under the action of buoyancy. If the wandering bubble is too small to approach the cavitation bubble size (The maximum diameter is less than 0.1 mm), the Bjerknes forces applied to it will be too large. The behavior of the too small wandering bubble will be more like a cavitation bubble and become a part of the cavitation structure. Statistics show that the diameter of the wandering bubbles rotating around the holding bubble array is about 0.2–0.4 mm in the ultrasonic field of 18.5 kHz. In this size range, the bubbles not only vibrates radially, but also fluctuates on the surface.

0.2–0.4 mm is a narrow size range. It is necessary to explore the origin of wandering bubbles. It is found that almost all the wandering bubbles originate from nearby ALF (Acoustic Lichtenberg Figure) cavitation structure (as shown in Fig. 5A,B,C. The yellow arrow indicates the direction of the cavitation bubble's movement). ALF structure are common in a cavitation field with relatively weak intensity [21].

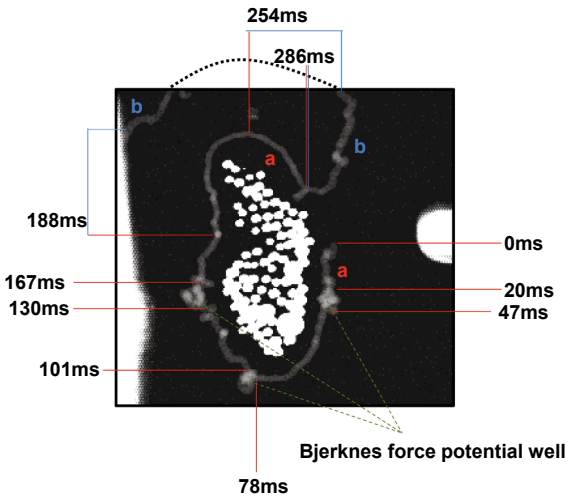

Fig. 6. The transformation of wandering bubble to holding bubble. A composite image of superimposing the snapshots from the video sequence. The width of the orbital trajectory is about 6.4 mm. The height of the orbital trajectory is about 11.6 mm. The rotation period is about 0.4 s. Average distance between the trajectory and the bubble array is about 1 mm. The output power of ultrasonic generating system is about 50 W.

Bubbles in ALF translationally move towards the pressure antinodes one after another form a dendritic structure (as shown the subfigure in the yellow dotted box in Fig. 5C). In the process of cavitation bubble translational movement, especially at the pressure antinode, a large number of cavitation bubbles merge. The coalescence of cavitation bubbles leads to the increase of air content and volume of the bubble. Finally, the bubble dominated by radial vibration (cavitation bubble) gradually transits to the bubble dominated by surface fluctuation (gas bubble). As the bubble volume increases, the Bjerknes force on the bubble decreases and the buoyancy increases [11]. As a result, the small gas bubble will escape the shackles of the cavitation cloud, move to

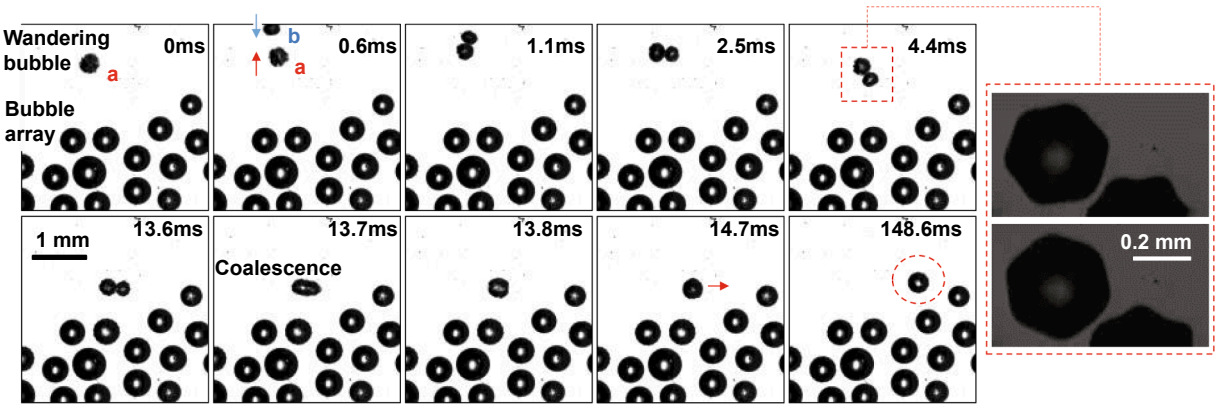

Fig. 7. The detailed process of the transformation of wandering bubble to holding bubble. The diameter of the holding bubble is 0.42–0.63 mm. The diameter of wandering bubble *a* is 0.32 mm. The diameter of wandering bubble *b* is 0.27 mm. The diameter of the bubble formed by the combination of bubble *a* and bubble *b* is 0.41 mm. The output power of ultrasonic generating system is about 50 W.

specific areas on the wall and become a wandering bubble (as shown in Fig. 5E, because the distance between the ALF cavitation structure and the bubble array is very long (about 10 cm), the shooting effect is not good, so only schematic diagram (instead of actual photos) was provided to show the whole process of the generation of wandering bubbles.). In fact, both the wondering bubbles and holding bubbles are "degas" bubbles, which is defined in reference [22].

It must be pointed out that the generation of wandering bubbles depends on the abundance of gas nuclei in the liquid. If there are few gas nuclei in the liquid, a large number of cavitation bubbles will still converge at the pressure antinode, but no wandering bubbles will be generated (as shown in Fig. 5D). The increasing amount of gas accumulated in the pressure antinode is dispersed with smaller microbubbles [23] (the radius of microbubbles is much smaller than the resonance radius at this frequency, and the Bjerknes force on them is also very small).

A wandering bubble does not rotate around a bubble array forever. It is found that almost all the wandering bubble rotating around a bubble array will stop moving and become a holding bubble by merging (as shown in Fig. 6). The wandering bubble (bubble *a*) rotate around a bubble array from $\tau = 0$ ms to $\tau = 286$ ms. When another wandering bubble (bubble *b*) appears ($\tau = 188$ ms), the two wandering bubbles merge and attach to the edge of the bubble array to become a part of it ($\tau = 286$ ms). The wandering bubble (whose radius is much larger than the resonance radius at ultrasonic frequency) is smaller than the holding bubble in the array, and the Bjerknes force on the wandering bubble is greater than that of the holding bubble. This is the reason why the wandering bubbles are more active than the holding bubbles. By merging with other wandering bubbles, the volume of the wandering bubbles increases, which reduces the Bjerknes force, weakens the activity, and makes them become holding bubbles. Wandering bubbles are also often merged with small holding bubbles located at the edge of the bubble array. There are three Bjerknes force potential well in Fig. 6, where the wandering bubble is confined to the well for a long time

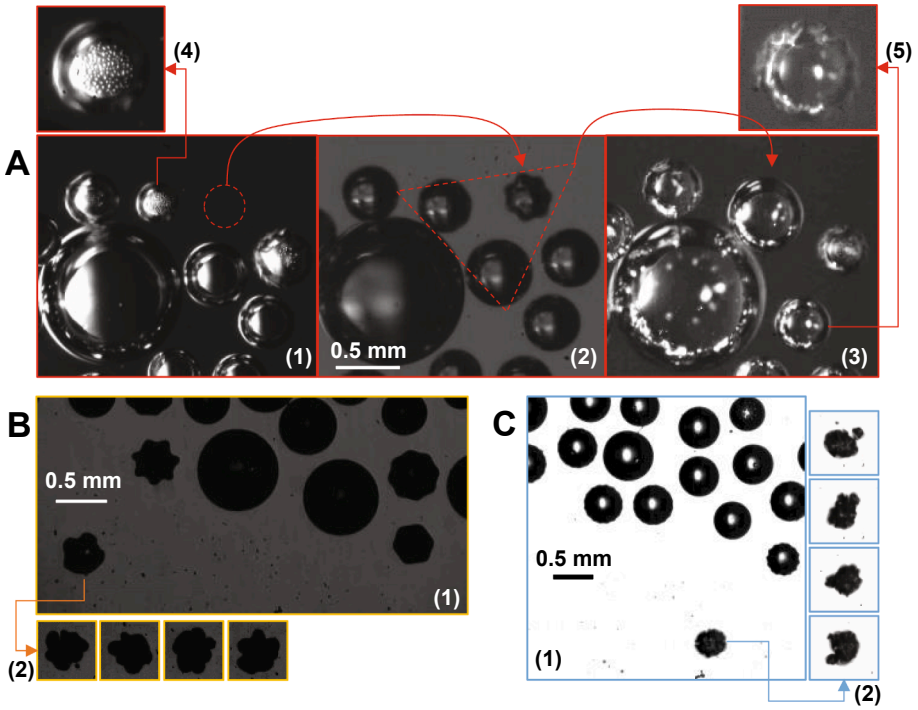

Fig. 8. Surface morphology of wandering bubble and holding bubble. (A) Surface morphology of holding bubbles. (B)(C) Surface morphology of a wandering bubble. The output power of ultrasonic generating system is about 50 W.

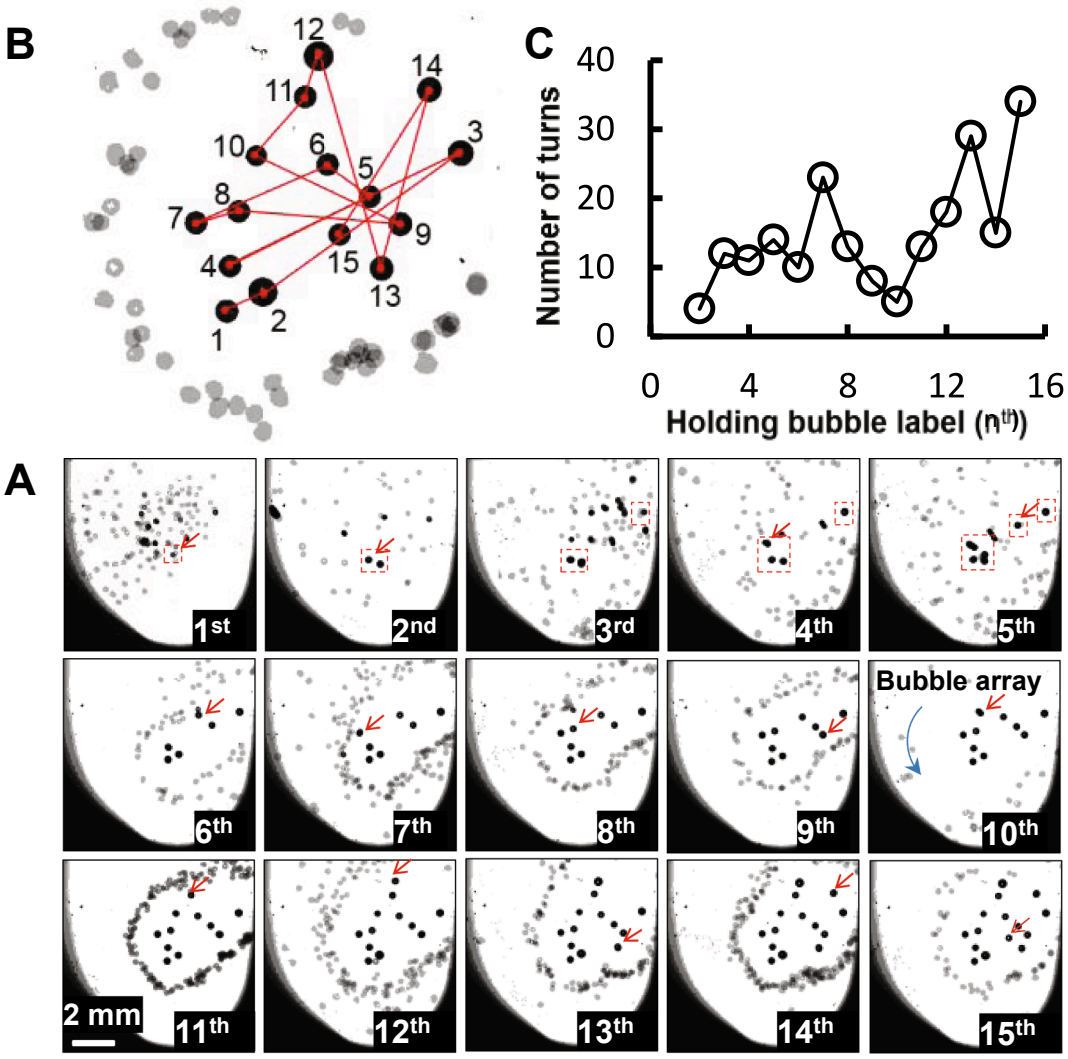

Fig. 9. The locations where the nth bubble in the array once appeared. (A) Composite images of superimposing the snapshots from the video sequence. (B) The order of appearance and spatial position of holding bubbles. (C) The number of turns before it becomes a holding bubble. The output power of ultrasonic generating system is about 50 W.

(20–40 ms).

A merging process of two wandering bubbles was photographed by a high-speed camera in a framing rate of 10,000 fps and an exposure time of 1/10000 s (as shown in Fig. 7). Unlike the merging of two cavitation bubbles (radial vibration), the two wandering bubbles (radial vibration + surface fluctuation) attract each other but do not merge immediately. The bubble *a* and bubble *b* coalesced after contacting 252 sound cycles (during contact, there is a liquid film between the two bubbles (as shown the subfigure in Fig. 7 in another experiment)). The radial vibration of the two wandering bubbles is in the same phase (attraction); the surface fluctuation of the two bubbles is anti-phase (repulsion), so the two bubbles are close to each other but do not merge. When the liquid film breaks, the merging process of the two wandering bubbles is similar to that of two ordinary gas bubbles. The surface tension dominates the merging process. After merging, the newly generated holding bubble may still move a little distance until it reach the position where the Bjerknes force is the least (when $\tau = 14.7$ ms, the bubble surface still vibrates (opaque in center), and when $\tau = 148.6$ ms, it does not vibrate at all (light transmission)).

Fig. 8 shows the surface morphology of wandering bubbles and holding bubbles in a larger magnification. Fig. 8A uses different lighting for the same scene. It can be seen that the shape of the holding bubbles is very regular. There are many micro droplets on the glass wall surface inside some holding bubbles (as shown in Fig. 8A(4)), which is caused by the fluctuation sputtering of the bubble surface. A new holding bubble appears in 8A(2). Because of its small size and large force, its surface fluctuates obviously. Then, the three nearby holding bubbles merge to form a larger holding bubble (as shown in Fig. 8A(3)). Different lighting effects are used in Fig. 8B and Fig. 8C. It can be seen that the surface fluctuation of wandering bubbles is very violent, resulting in irregular shape and even splitting of small bubbles [20,24].

As more wandering bubbles become holding bubbles, the bubble array is gradually developed. Fig. 9 shows the development of a bubble array (from the 1st bubble to the 15th bubble). Each subfigure in Fig. 9A is a superposition of many high-speed photographs (50 fps), showing the locations where the nth wandering bubble from its first appearance to its final residence. It can be seen that the positions of the first few wandering bubbles were scattered, and the final holding positions were also relatively random, indicating that their circular motion was not stable. With the increase of holding bubbles, the positions where wandering bubbles once appeared are more and more concentrated around the array (as shown in Fig. 9A), the number of rotations before it becomes a holding bubble also tends to increase (as shown in Fig. 9C), and the position distribution of holding bubbles is concentrated in the periphery (as shown in Fig. 9B). These show that the circular motion of wandering bubbles is more and more stable. The development of the bubble array

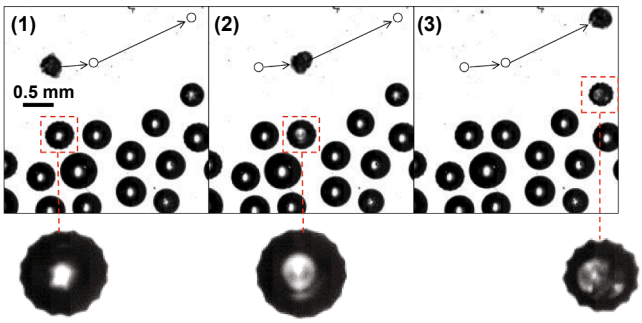

Fig. 10. The effect of a wandering bubble on holding bubbles. The output power of ultrasonic generating system is about 50 W.

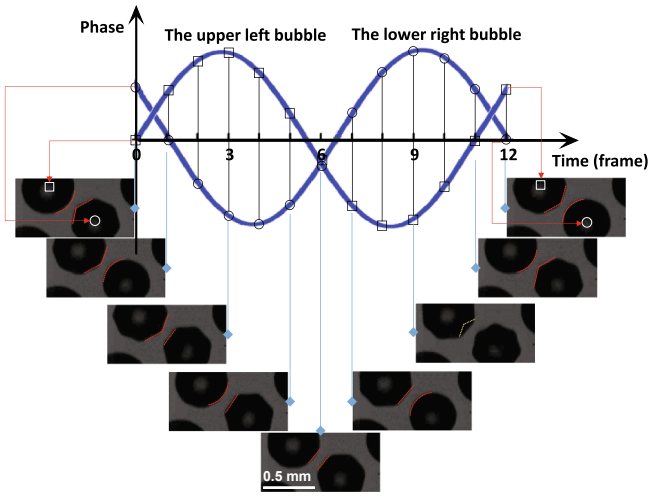

Fig. 11. Surface fluctuation of adjacent holding bubbles in a bubble array in a cycle (Frame rate: 100,000 fps). The output power of ultrasonic generating system is about 50 W.

shows that the bubble array has a great influence on the motion and residence of wandering bubbles.

The wandering bubble also has a great influence on the holding bubbles. When a wandering bubble approaches a holding bubble, the surface of the holding bubble will fluctuate obviously (as shown in Fig. 10). When the surfaces of two neighboring holding bubbles fluctuate, the vibration of the two bubbles has a stable phase relationship (as shown in Fig. 11). Their surface fluctuation period is 110 μs, which is twice the sound period (54 μs), holding bubbles are oscillating sub-harmonically. The diameter of the two adjacent bubbles is the same, and their shapes are constantly changing between a circle and an octagon. The larger the bubble diameter, the more sides the polygon will be formed [25] (for example, the bubble in Fig. 10 (1) (2) is 16 sided, and the bubble in Fig. 10 (3) is 14 sided). The phase of the surface fluctuation of the two bubbles is roughly opposite (1/11 cycle deviation). This fluctuation coupling ensures that the thickness of the liquid layer between the two bubbles and the pressure in the liquid layer remain unchanged during the bubble vibration. This is why the holding bubbles are regularly arranged and rarely coalesce with each other unless there is a large disturbance, such as a sudden closing or opening of the transducer.

The circular motion of submillimeter-sized bubbles attached to a boundary in an ultrasonic field are investigated experimentally by high-speed photography and image analysis. Different from the circular motion of suspended bubbles in water, gas bubbles attached to a boundary will rotate around a regularly arranged bubble array. The orbital trajectory of wandering bubble is not regular circular or elliptical (the trajectory is approximately the contour of the bubble array), the trajectory is not stable (the trajectory of each cycle does not coincide), and the trajectory is not smooth (the trajectory curve has many singular points), because of the acoustic field radiated by the holding bubbles in the array and the boundary effect of vibrating bubbles. The diameter of the wandering bubbles is about 0.2–0.4 mm in the ultrasonic field of 18.5 kHz. In this size range, the bubbles not only vibrates radially, but also fluctuates on the surface. The primary Bjerknes drives the wandering bubbles to move towards the bubble array, while the secondary Bjerknes force repels the wandering bubbles. The balance between the two forces ensures a stable distance between the wandering bubbles and the bubble array. The circling bubbles go through nodal line and anti-nodal region in turn. Almost all the wandering bubbles originate from nearby ALF cavitation cloud, and almost all the wandering bubble rotating around a bubble array will stop moving and become a holding bubble. With the increase of holding bubbles in the array, the circular motion becomes more stable. The bubble array has a great influence on the motion and residence of wandering bubbles, and the wandering bubble also has a great influence on the holding bubbles. Holding bubbles are oscillating sub-harmonically, and the phase of the surface fluctuation of the two bubbles is roughly opposite, which ensures that the distance between two adjacent bubbles is stable.

CRediT authorship contribution statement

Bai Lichun: Methodology, Formal analysis, Investigation, Writing - original draft. **Sun Jinguang:** Conceptualization, Supervision. **Gao Yandong:** Software. **Xu Weilin:** Methodology, Supervision. **Zeng Zhije:** Visualization. **Ma Yuhang:** Software. **Bai Lixin:** Investigation, Conceptualization, Methodology, Supervision.

Declaration of Competing Interest

The authors declare that they have no known competing financial interests or personal relationships that could have appeared to influence the work reported in this paper.

Acknowledgments

This work was supported by the National Natural Science Foundation of China (No. 11874062, No. 11674350), the National Key Research and Development Project (No. 2018YFB1403303).

References

[1] W.L. Shew, J.F. Pinton, Dynamic model of bubble path instability, Phys. Rev. Lett. 97 (2006), 144508.
[2] L. Bai, J. Yan, L. Bai, Z. Zeng, Y. Ma, Cinematographic observation of the deformation of an antibubble when aspark-induced cavitation bubble oscillates in its vicinity, Colloids Surf. A 592 (2020), 124606.
[3] F.R. Young, Cavitation, McGraw-Hill Book Company, London, 1989.
[4] P. Tho, R. Manasseh, A. Ooi, Cavitation microstreaming patterns in single and multiple bubble systems, J. Fluid Mech. 576 (2007) 191–233.
[5] L. Bai, W. Xu, C. Li, Y. Gao, The counter jet formation in an air bubble induced by the impact, J. Hydrodyn. Ser. B 23 (2011) 562–569.
[6] Y. Tomita, A. Shima, T. Sugiu, Mechanisms of impulsive pressure generation and damage pit formation by bubble collapse, J. Fluid Mech. 169 (1986) 535–564.
[7] M. Versluis, D.E. Goertz, P. Palanchon, I.L. Heitman, S. van der Meer, B. Dollet, N. de Jong, D. Lohse, Microbubble shape oscillations excited through ultrasonic parametric driving, Phys. Rev. E 82 (2010), 026321.
[8] T.-H. Kim, H.-Y. Kim, Disruptive bubble behaviour leading to microstructure damage in an ultrasonic field, J. Fluid Mech. 750 (2014) 355–371.
[9] T.G. Leighton, A.J. Walton, M.J.W. Pickworth, Primary Bjerknes forces, Eur. J. Phys. 11 (1) (1990) 47–50.
[10] J.R. Blake, U. Parlitz, R. Mettin, S. Luther, I. Akhatov, M. Voss, W. Lauterborn, Spatio-temporal dynamics of acoustic cavitation bubble clouds, Philos. Trans. R. Soc. Lond. A 357 (1751) (1999) 313–334.
[11] R. Mettin, Bubble structures in acoustic cavitation, in: AA. Doinikov (Ed.), Bubble and Particle Dynamics in Acoustic Fields: Modern Trends and Applications, Reaserch Signpost, Kerala, 2005, pp. 1-36.
[12] T. Kodama, K. Takayama, N. Nagayasu, The dynamics of two air bubbles loaded by an underwater shock wave, J. Appl. Phys. 80 (10) (1996) 5587–5592.

[13] D.L. Miller, Stable arrays of resonant bubbles in a 1-MHz standing-wave acoustic field, J. Acoust. Soc. Am. 62 (1) (1977) 12–19.
[14] T. Barbat, N. Ashgriz, Planar dynamics of two interacting bubbles in an acoustic field, Appl. Math. Comput. 157 (3) (2004) 775–824.
[15] J. Rensen, D. Bosman, J. Magnaudet, C.D. Ohl, A. Pros-peretti, R. Togel, M. Versluis, D. Lohse, Spiraling Bubbles: How Acoustic and Hydrodynamic Forces Compete, Phys. Rev. Lett. 86 (21) (2001) 4819.
[16] M. Shirota, K. Yamashita, T. Inamura, Orbital motions of bubbles in an acoustic field, Nonlinear Acoustics: State-of-the-Art and Perspectives (ISNA 19), Amer. Inst. Phys. Melville (2012).
[17] C. Desjouy, P. Labelle, B. Gilles, J.C. Bera, C. Inserra, Orbital trajectory of an acoustic bubble in a cylindrical resonator, Phys. Rev. E 88 (2013), 033006.
[18] C. Desjouy, P. Labelle, B. Gilles, J.C. Bera, C. Inserra, Acoustic bubble behavior in a standing wave field, J. Acoust. Soc. Am. 133 (2013) 3277.
[19] Y. TOMITA, P.B. ROBINSON, R.P. TONG, J.R. BLAKE, Growth and collapse of cavitation bubbles near a curved rigid boundary, J. Fluid Mech. 466 (2002) 259–283.
[20] L. Bai, W. Xu, F. Zhang, N. Li, Y. Zhang, D. Huang, Cavitation characteristics of pit structure in ultrasonic field, Sci. China Ser. E 52 (7) (2009) 1974–1980.
[21] L. Bai, W. Xu, J. Deng, C. Li, D. Xu, Y. Gao, Generation and control of acoustic cavitation structure, Ultrason. Sonochem. 21 (5) (2014) 1696–1706.
[22] K. Yasui, Influence of ultrasonic frequency on multibubble sonoluminescence, J. Acoust. Soc. Am. 112 (4) (2002) 1405–1413.
[23] R. Mettin, S. Luther, C.-D. Ohl, W. Lauterborn, Acoustic cavitation structures and simulations by a particle model, Ultrason. Sonochem. 6 (1-2) (1999) 25–29.
[24] L.-X. Bai, W.-L. Xu, Z. Tian, N.-W. Li, A high-speed photographic study of ultrasonic cavitation near rigid boundary, J. Hydrodyn. Ser. B 20 (5) (2008) 637–644.
[25] P. Wu, L. Bai, W. Lin, D. Xu, C. Li, Surface oscillations and fragmentation of bubbles in an acoustic field, Proc. Mtgs. Acoust. 32 (2017), 045004.